Applied Surface Science 414 (2017) 424–434

Contents lists available at ScienceDirect

Applied Surface Science

journal homepage: www.elsevier.com/locate/apsusc

Enhancement of p-nitrophenol adsorption capacity through N_2-thermal-based treatment of activated carbons

S. Álvarez-Torrellas [a,b,*], M. Martin-Martinez [b], H.T. Gomes [b], G. Ovejero [a], J. García [a,b]

[a] Grupo de Catálisis y Procesos de Separación (CyPS), Departamento de Ingeniería Química, Facultad de Ciencias Químicas, Universidad Complutense de Madrid, Avda. Complutense s/n, 28040 Madrid, Spain

[b] Laboratory of Separation and Reaction Engineering – Laboratory of Catalysis and Materials (LSRE-LCM), Department of Chemical and Biological Technology, School of Technology and Management, Polytechnic Institute of Bragança, Campus de Santa Apolónia, 5300-253 Bragança, Portugal

ARTICLE INFO

Article history:
Received 27 December 2016
Received in revised form 27 February 2017
Accepted 6 April 2017
Available online 14 April 2017

Keywords:
Activated carbon
Adsorption
Fixed-bed column
4-Nitrophenol

ABSTRACT

In this work several activated carbons showing different textural and chemical properties were obtained by chemical and physical activation methods, using a lignocellulosic material (peach stones) as precursor. The activated carbon resulting from the chemical activation, namely as CAC, revealed the best textural properties (S_{BET} = 1521 $m^2\ g^{-1}$, pore volume = 0.90 $cm^3\ g^{-1}$) and an acidic character. It was found that the activated carbon obtained at 300 °C (under air atmosphere, PAC_air), and those synthesized at 750 °C in presence of N_2 flow with bubbling of water/12 M H_3PO_4 solution (PAC_N_2(H_2O)/PAC_N_2(H_3PO_4)), respectively, revealed worse textural properties, compared to CAC. Two functionalization treatments, by using sulphuric acid at boiling temperature (PACS) and nitric acid-urea-N_2 heating at 800 °C (PAC-NUT), were applied to PAC_air, in order to enhance the adsorption ability of the carbon material. Several techniques were carried out to characterize the physical and chemical properties of the obtained carbon materials. The modification treatments had influence on the carbon surface properties, since the nitric acid-urea-N_2 heating treatment led to a carbon material with highly-improved properties (S_{BET} = 679 $m^2\ g^{-1}$, pH_{IEP} = 5.3).

Accordingly, the original and modified-carbon materials were tested as adsorbents to remove 4-nitrophenol (4-NP), assessing batch and fixed-bed column adsorption tests. PAC-NUT carbon offered the best adsorption behavior (q_e = 234 mg g^{-1}), showing a high ability for the removal of 4-NP from water.

1. Introduction

Nitro-aromatic compounds are a class of compounds with one or more nitro substituents. Among them, 4-nitrophenol (4-NP) is a hazardous pollutant mainly produced during chemical processes, such as petrochemical manufacturing, oil refining, rubber, wood preservation operations, pulp and paper mills as well as in the production of pesticides, paints and plastics [1]. The presence of phenol and its derivatives in the aquatic environment has become a great concern in recent years due to their increasing discharge, toxic nature and potential adverse effects on the receiving water bodies [1,2].

Phenolic compounds are known to have a toxic effect on aquatic life, plants and even human health. Ingestion of phenol at a concentration level of 10–240 mg L^{-1} for a long period causes mouth sores, diarrhea, excretion of dark urine and impaired vision. Accordingly, the lethal blood concentration for phenol is around 4.7–130 mg L^{-1}.

Due to its toxicity, even at low concentrations, phenolic compounds have been classified as priority pollutants by the U.S. Environmental Protection Agency (EPA). Per the recommendation of the World Health Organization (WHO), the threshold concentration of phenol in drinking water should fall below 1.0 μg L^{-1}. Therefore, the USEPA recommends a maximum level of 1 μg mL^{-1} of total phenolic compounds in water supplies.

Due to its harmful effects, wastewaters containing phenolic compounds should be specifically treated before being discharged to the receiving water bodies.

The tertiary treatments for the removal of persistent pollutants from wastewater include advanced oxidation processes (AOPs) with their variations (ozone, ultraviolet radiation, gamma radiation), membrane bioreactors, micro/nanofiltration and adsorption

* Corresponding author at: Grupo de Catálisis y Procesos de Separación (CyPS), Departamento de Ingeniería Química, Facultad de Ciencias Químicas, Universidad Complutense de Madrid, Avda. Complutense s/n, 28040 Madrid, Spain.
E-mail addresses: satorrellas@ucm.es (S. Álvarez-Torrellas), mariamartin@ipb.pt (M. Martin-Martinez), htgomes@ipb.pt (H.T. Gomes), govejero@ucm.es (G. Ovejero), jgarciar@ucm.es (J. García).

http://dx.doi.org/10.1016/j.apsusc.2017.04.054
0169-4332/

[3,4]. Adsorption is an effective separation process due to its simple design, operation flexibility, suitability for batch and continuous mode, possibility of regeneration and reuse of the saturated adsorbents and low capital costs [5]. The selection of the adsorbent for each specific application is a critical aspect in the adsorption processes. Zeolites, due to their relatively high surface area and tailored-porosity (micro, meso and macro pores) have demonstrated usefulness as adsorbent materials for the removal of organic pollutants [6]. Accordingly, metal oxides, such as MnO, have been widely used for the depletion of hazardous and undesirable compounds from wastewater. Therefore, metal oxides are often characterized by small specific surface area, and consequently, they could be modified by several treatments in order to obtain better adsorption properties. For example, Mn_xO_y-SiO_2 mixed oxides materials show better textural properties and adsorption affinity than manganese oxides, exhibiting higher adsorption capacity [7].

In general, activated carbons offer a high adsorption performance for a wide range of organic and inorganic pollutants due to their high surface area and pore volume [8]. Low-cost, quite abundance, renewability, and high lignocellulosic content of agricultural biomass make them promising precursors for cost-effective activated carbons [9]. A wide number of lignocellulosic residues, such as bamboo, wood, nuts, sawdust, cherry stones, rice husk, peach stones [10], coffee wastes, potato peels, almond shells [11] and peanut shells [10,11], among many others, are of particular interest as by-products from food processing industries, in order to obtain activated carbons with good mechanical strength and a well-developed porous structure.

Physical and chemical methods have been adopted for the conversion of these biomass wastes to activated carbons [12]. Physical activation involves the pyrolysis of the carbonaceous precursor at high temperatures followed by activation of the char in the presence of an oxidizing gas (CO_2 or water steam) [13,14]. In chemical activation, the raw material is firstly impregnated with strong activating agents such as $ZnCl_2$, H_2SO_4, NaOH, K_2CO_3, H_3PO_4, KOH, among others, followed by thermal activation at temperatures ranging from 400 to 600 °C [15].

In the chemical activation method, the dehydrating effect of the activating agent, for example, H_3PO_4 solution, hinders the formation of tar, leading to higher yield and the possibility to use low activation temperatures to produce higher grade carbons [16]. Both in physical and chemical reactions, it is necessary the activation step to enhance the pore volume, pore diameter and surface area of the resulting material [17]. In general, longer activation times are favorable for the development of higher micro porosity and specific surface area.

The textural and chemical properties of the activated carbon mainly condition the specific application and the results obtained. Generally, for liquid-phase adsorption, a high surface area is desirable and a mesoporous texture enhances the diffusion of the pollutant within the porous structure of the adsorbent [18].

In the present work, activated carbons from peach stones have been prepared as follows: (i) chemical activation: impregnation with 12 M $H_3PO_{4(s)}$ and further thermal treatment (400 °C, 4 h, air flow); the resulting material was named as CAC; (ii) physical activation by the following methods: (1) activation in N_2 presence (800 °C, 4 h) followed by treatment in air flow (300 °C, 1 h); carbon namely as PAC_air; (2) activation under N_2 atmosphere (600 °C, 1 h) and further under N_2 saturated in H_2O (750 °C, 6 h); material namely as PAC_N_2(H_2O); (3) activation under inert atmosphere (600 °C, 1 h) and subsequently it was annealed in N_2 saturated with 12 M $H_3PO_{4(s)}$ (750 °C, 6 h); the resulting material was named as PAC_N_2(H_3PO_4). Additionally, PAC_air was functionalized in order to enhance the adsorption ability of the carbon material. The carbon was treated with concentrated H_2SO_4 solution (200 °C, 3 h), resulting in PACS activated carbon. Accordingly, the basic functionalization to obtain PAC-NUT carbon consisted of the treatment of PAC_air with 5 M $HNO_{3(s)}$ (83 °C, 3 h), further it was treated with 1 M urea solution at autogenous pressure (200 °C, 2 h) and the resulting material was annealed at 800 °C for 4 h.

The textural, chemical and morphological properties of all the tested carbon materials were studied. They were further tested as adsorbents regarding kinetic and equilibrium 4-NP adsorption tests both in batch and fixed-bed column operation.

2. Experimental

2.1. Reactants

Peach stones were collected from a local agricultural company, producing peach cans in syrup, being the fruit stones a biomass waste daily originated.

4-Nitrophenol (4-NP, $O_3NC_6H_5$, 98 wt.%) and phosphoric acid (85 wt.%) were purchased from Sigma–Aldrich. Sulphuric acid (98 wt.%) was obtained from Panreac. Nitric acid (69.5 wt.%) and acetonitrile (HPLC grade) were provided by Carlo Erba. Urea (65 wt.%) was purchased from Riedel-de-Haën. Methanol (HPLC grade) and glacial acetic acid (analytical reagent grade) were obtained from Fisher chemical. All reagents were used as received. Ultrapure water was used throughout the research.

2.2. Preparation of the activated carbons

In the chemical activation method, firstly, an impregnation step was carried out placing 30 g of precursor (0.5–1.0 mm) with 12 M $H_3PO_{4(s)}$ in a round-bottom flask reactor at 85 °C for 6 h. After that, the solid was filtered and carbonized in a vertical quartz reactor under flowing air (50 $cm^3\ min^{-1}$) at 400 °C for 4 h (5 °C min^{-1}). The resulting carbon was thoroughly washed several times with ultrapure water until a pH close to neutrality was reached. Then, the activated carbon was dried overnight and it was sieved at the required particle size range (100–250 μm) [19]. The resulting material was namely as CAC.

Physical activation method in order to obtain PAC_air material was carried out as follows, adapting the method developed by Ribeiro et al. [20]: 30 g of precursor was annealed (100 $cm^3\ min^{-1}$) in a vertical quartz reactor at 120, 400 and 600 °C during 1 h at each temperature, and finally at 800 °C for 4 h (2 °C min^{-1}). The resulting material was further activated under air flow (100 $cm^3\ min^{-1}$) for 1 h at 300 °C.

Finally, PAC_N_2(H_2O) and PAC_N_2(H_3PO_4) activated carbons were obtained as the following method: 30 g of precursor was heated under N_2 flow (100 $cm^3\ min^{-1}$) from room temperature to 600 °C and maintained for 1 h (5 °C min^{-1}). The activation of the obtained char was carried out at 750 °C (15 °C min^{-1}) under N_2 saturated with water or 12 M $H_3PO_{4(s)}$, maintaining the temperature for 6 h [21].

2.3. Modification of the activated carbon

PAC_air activated carbon was modified by two functionalization treatments in order to study the behavior of the modified materials on 4-NP adsorption, following the procedures reported elsewhere by Gomes et al. and Rocha et al. [22,23], respectively.

Firstly, a suspension containing 50 g L^{-1} of PAC_air in concentrated $H_2SO_{4(s)}$ (18 M) was kept for 3 h at 200 °C in a 250 mL round-bottom flask; the resulting solids were thoroughly washed with ultrapure water until neutrality and further dried in an oven overnight. This activated carbon was namely as PACS.

In the second procedure, a suspension of PAC_air material (50 g L^{-1}) was treated using 5 M HNO_3 solution for 3 h at boiling temperature (83 °C); then, the carbon was washed until neutrality

of the rinsing waters and further dried overnight. 2 g of this material was put in contact to 50 mL of urea solution (1 M) in a 125 mL stainless steel autoclave batch reactor under autogenous pressure at 200 °C for 2 h. Finally, a thermal treatment was applied to the recovered solids, under N_2 flow (100 cm^3 min^{-1}) at 120, 400 and 600 °C during 1 h at each temperature and 800 °C for 4 h, resulting in the final material (PAC-NUT).

2.4. Characterization of the activated carbons

2.4.1. Textural characterization

The textural characterization of the activated carbons was studied by N_2 adsorption–desorption isotherms at 77 K in a Micromeritics ASAP 2020 equipment. The specific surface area (S_{BET}) was calculated by using BET equation [24] in the range of P/P^0 = 0.05–0.15, external surface area (S_{ext}) was estimated by *t*-plot method and Dubinin–Radushkevich equation was used to calculate micro pore volume (V_0) [25]. Meso pore volume was determined by subtracting the value of V_0 from the total N_2 amount adsorbed at P/P^0 = 0.95 [26]. Pore size distributions (PSD) of the tested carbons were obtained by density functional theory (DFT) method.

2.4.2. Surface chemistry characterization

Chemical surface characterization was performed by Fourier Transformed Infrared Spectroscopy (FTIR), using a Thermo Nicolet FTIR spectrophotometer. Infrared spectra were recorded in a wavelength range ranging from 400 to 4600 cm^{-1}.

The point of zero charge (pH_{PZC}) of the synthesized activated carbons was determined following a pH titration procedure. 20 mL of NaCl 0.01 M solution was poured into several 25 mL-vessels. pH within each vessel was adjusted to a value between 2.5 and 11 by addition of HCl 0.02 M or NaOH 0.02 M solutions. Then, 0.05 g of sample was added to the vessels and they were located in an orbital shaker under agitation at 320 rpm. The final pH was measured after 48 h, using a calibrated pH meter (Model GLP 21; Crison Instruments SA; Barcelona, Spain) with an accuracy of ±0.01 pH. A Crison 5015T electrode, with two ceramic diaphragms was used. pH_{PZC} value is defined as the point where the pH final curve vs. pH initial crosses the main diagonal of the plot [27]. The isoelectric point (pH_{IEP}) of the samples was determined by electrophoretic migration measurements using a Zetasizer Nano ZS equipment (Malvern Instruments). A suspension of 0.050 g of sample (10–20 μm of particle size) in 20 mL of ultrapure water was used for the measurements. pH solution was modified with either 0.1 M HCl or NaOH solutions. pH_{IEP} value was calculated by the graphical representation of zeta potential values versus pH of solution.

Elemental composition of the activated carbons (C, H, N and S, %) was determined by elemental microanalysis using a LECO CHNS-932 analyzer. Activated carbon sample (0.6–1.6 mg) was held in a furnace at 1000 °C, where the combustion of the sample occurred. Finally, thermogravimetric analyses (TG) of the activated carbons were performed. Samples were measured in an EXTAR 6000 Seiko thermal analyzer, operating with N_2 flow (100 cm^3 min^{-1}), and heating from 35 to 900 °C at a heating rate of 10 °C min^{-1}.

2.4.3. Morphological characterization

Morphological studies were carried out with a JEOL JSM 6400 microscope, equipped with a thermoionic cathode and a 25 kV detector. Previously, carbon samples were coated with a gold layer, using a Balzers SCD004 apparatus, for 180 s.

2.5. Equilibrium adsorption studies

The adsorption rate and the equilibrium time are strongly dependent on the adsorbent particle size. The activated carbon samples were ground and sieved; only the size fraction smaller than 100 μm was used in the adsorption experiments.

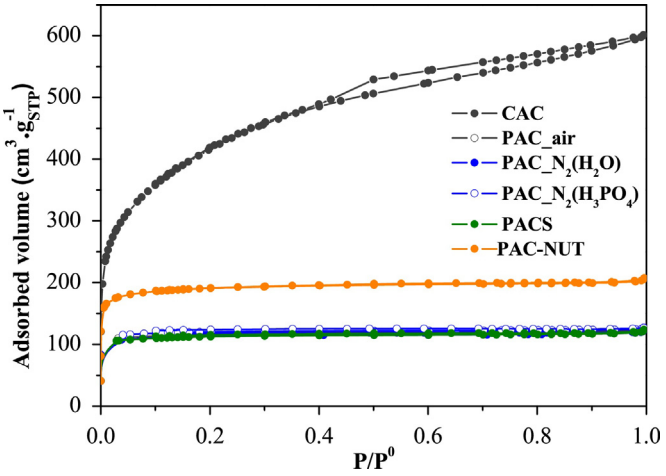

Fig. 1. N_2 adsorption–desorption isotherms at 77 K of the tested adsorbents.

In order to study the kinetic 4-NP adsorption, 60 mg of adsorbent was placed in contact to 25 mL of contaminant solution (C_0 = 100 mg L^{-1}) in Deltalab plastic vessels in an orbital shaker (LabMate). Temperature and stirring rate were constant in the experiments (30 °C, 250 rpm). At the required interval times, the vessels were removed, solution was filtered by using 0.45 μm-nylon syringe filters and 4-NP concentration was analyzed in a High Liquid Pressure chromatograph (Jasco), equipped with a UV/vis detector (UV-2075 Plus) and a quaternary gradient pump (PU-2089 Plus) for solvent delivery. The analyses were carried out using a Kromasil 100-5-C18 column (15 cm × 4.6 mm; 5 μm particle size), working at room temperature. The mobile phase used was methanol (3% acetic acid, 1% acetonitrile):ultrapure water (3% acetic acid) (40:60, v/v) at a flow rate of 1 mL min^{-1}.

In the equilibrium adsorption tests, different weights of adsorbent (5–800 mg) were placed in contact to 25 mL of 4-NP solution (C_0 = 100 mg L^{-1}) in a LabMate orbital shaker (30 °C, 250 rpm). After reaching the equilibrium time, samples were filtered and analyzed as detailed above. The analyses were carried out in duplicate; additionally, blank tests were accomplished in order to evaluate possible contaminant removal by other mechanisms, obtaining negative results.

2.6. Fixed-bed column adsorption experiments

Adsorption tests in fixed-bed column were performed using glass tubes adapted with a metallic layer at the bottom as support of the adsorbent and re-filled with glass balls in order to avoid dead volume and preferential channels in the bed. 0.8 g of PAC_air carbon (particle size: 106–250 μm) was used in the experiments. 4-NP solution (C_0 = 10.0 mg L^{-1}) was pumped using a peristaltic pump at a selected volumetric flow rate (Q = 1.33 and 2.50 mL min^{-1}), operating in *down-flow* mode. 1.5 mL effluent samples were periodically collected and analyzed by using high performance liquid chromatography (HPLC), as described above.

3. Results and discussion

3.1. Characterization of the activated carbons

3.1.1. Textural characterization of the activated carbons

N_2 adsorption–desorption isotherms at 77 K and pore size distributions (PSD) of the tested activated carbons are depicted in Fig. 1

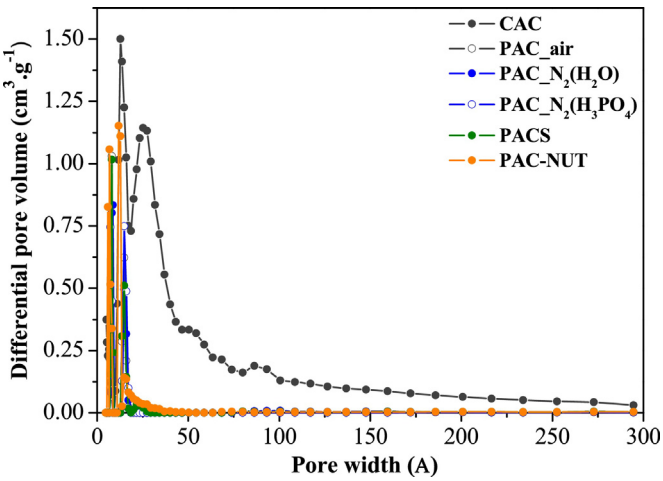

Fig. 2. Pore size distributions of the tested adsorbents.

and Fig. 2, respectively. S_{BET}, S_{ext}, micropore (V_0) and mesopore (V_m) volumes were determined.

CAC activated carbon presented a highly developed porosity network of micropores in combination with a high percentage of mesopores, offering much higher amount of adsorbed N_2 than the physically-activated activated carbons, which can be classified as strictly microporous materials. Thus, PAC_air, PAC_N_2(H_2O) and PAC_N_2(H_3PO_4) samples presented a strong microporous nature, with lower S_{BET} and V_m than CAC activated carbon (S_{BET} CAC/PAC_air = 1521/412 $m^2\,g^{-1}$; V_m = 0.379/0.004 $cm^3\,g^{-1}$) (Table 1).

CAC N_2 adsorption–desorption isotherm could be classified as Type I–IV, according to IUPAC classification [28], since a large mesoporous percentage is contributing on its porous structure. The presence of a hysteresis loop (Type H4) at high P/P^0 values (0.40–0.95) is suggesting the existence of abundant mesoporosity, associated to capillary condensation occurring in the mesopores. On the other hand, both physically-activated carbons and modified-materials N_2 adsorption isotherms could be classified as Type I, indicative of strictly microporous materials.

The mesoporous character of CAC activated carbon was confirmed in the PSD diagrams (Fig. 2), showing a pore diameter ranging from 27 to 50 Å, while the other microporous carbons had an average pore diameter smaller than 15 Å.

Textural properties of PACS material were not modified in a great extent, comparing to the original carbon (PAC_air). Thus, an increasing in the specific surface area and pore volume was observed in PAC-NUT carbon (S_{BET} = 679 $m^2\,g^{-1}$, V_{Total} = 0.309 $cm^3\,g^{-1}$) (Table 1). This behavior may be attributed to the removal of the main containing of the oxygenated surface functionalities, increasing the accessible carbon surface area for N_2 molecules [23].

3.1.2. Chemical surface characterization of the activated carbons

The chemical surface properties of the tested activated carbons were studied through elemental composition, FT-IR, point of zero charge (pH_{PZC}) and isoelectric point (pH_{IEP}) measurements. Both pH_{PZC} and pH_{IEP} values showed that CAC activated carbon presents higher surface acidity than PAC_air, being these results in accordance to those obtained in the elemental microanalysis (high O% composition and O/C ratio of CAC sample, this latter indicative of the polarity of the carbon materials [29]) (Table 2). Accordingly, as it can be expected, results showed that PAC_N_2(H_3PO_4) carbon is offering a slightly more acidic character than PAC_N_2(H_2O). Thus, the modified-activated carbons (PACS, PAC-NUT) were the most acidic and basic carbons, respectively, obtained in this study (pH_{IEP} PACS/PAC-NUT = 1.2/5.3).

Meanwhile, as it has been reported by León y León and Radovic [30], the difference observed between pH_{PZC} and pH_{IEP} values could be interpreted as a measurement of the charges distribution at the carbon surface. Positive values of $\{pH_{PZC} - pH_{IEP}\}$ are indicative of more negatively charged external than internal particle surfaces, this is, a heterogeneous distribution of the surface charges. This was observed in all the tested materials (Table 2).

FT-IR spectra of the activated carbons (Fig. 3a and b) revealed the absorption bands characteristic of the carbonaceous materials. Absorption spectra of CAC activated carbon (Fig. 3a) show the highest intensity in the absorption bands (phenolic and carbonyl groups), due to its high acidic character, compared to more basic activated carbons (PAC materials). Accordingly, FT-IR spectrum of PACS showed the incorporation of a high amount of oxygenated groups on the carbonaceous surface. Low intensity in the absorption bands was observed in PAC-NUT FT-IR spectrum, attributed to the removal of a high quantity of oxygenated-functionalities during the thermal treatment.

The absorption band at ~3400 cm^{-1} is characteristic of the O—H stretching vibration. Thus, the vibration at 1731 cm^{-1} (PACS) can be attributed to the C=O vibration of carbonyl in carboxylic or ester groups. The band at 1118 cm^{-1} could be associated to C—O bonding and the absorption peaks at ~1340 cm^{-1} seems to be responsible of the lactone groups, at ~1645 cm^{-1} to the conjugated —C=O groups and at ~1560 cm^{-1} and 1645 cm^{-1} to the carbonate functionalities.

The main differences found in FT-IR spectra of PAC_air and PACS are mainly observed at 3400, 1731, 1118 and 1340 cm^{-1} absorption bands. These results are in accordance to the data reported in the literature about characterization of activated carbons from lignocellulosic wastes [31–33].

In the thermogravimetric analysis of the tested carbon materials, shown in Fig. 4, could be observed a mass loss due to water steam ranging from 1.0 to 7.5% at temperature lower than 100 °C.

Both physically-activated carbons and PAC-NUT exhibited high thermal stability, showing only a mass loss in the range from 4 to 18% at 900 °C, indicating a complete degradation of the lignocellulosic materials during the carbonization and further activation procedures. Meanwhile, CAC and PACS materials showed a low thermal stability, with mass loss up to 37.5 and 47.5%, respectively. This could be attributed to the presence of acid solutions on the carbons surface, which decompose at lower temperatures than those at the acidic functionalities incorporated into the inner porous structure of the other carbons. These results are in agree-

Table 1
Textural properties (specific surface area, external surface area, total pore volume, micropore volume and mesopore volume) of the tested carbonaceous materials.

Carbon	S_{BET} ($m^2\,g^{-1}$)	S_{ext} ($m^2\,g^{-1}$)	V_{Total} ($cm^3\,g^{-1}$)	V_0 ($cm^3\,g^{-1}$)	V_m ($cm^3\,g^{-1}$)	V_m/V_{Total}
CAC	1521	1172	0.902	0.522	0.379	0.579
PAC_air	412	60	0.186	0.182	0.004	0.978
PAC_N_2(H_2O)	403	58	0.182	0.178	0.0038	0.978
PAC_N_2(H_3PO_4)	428	57	0.191	0.189	0.002	0.990
PACS	401	62	0.181	0.177	0.004	0.978
PAC-NUT	679	110	0.309	0.297	0.012	0.961

Table 2
Elemental microanalysis, point of zero charge and isoelectric point of the tested carbonaceous materials.

Carbon	N (%)	C (%)	H (%)	O (%)	S (%)	O/C ratio	pH_{PZC}	pH_{IEP}	$\{pH_{PZC} - pH_{IEP}\}$
CAC	0.33	68.70	3.91	27.04	0.02	0.394	4.3	1.9	2.4
PAC_air	0.63	84.68	1.69	12.98	0.02	0.153	5.9	2.5	3.4
PAC_N_2(H_2O)	0.77	90.83	1.42	6.96	0.02	0.077	6.4	2.4	4.0
PAC_N_2(H_3PO_4)	0.69	88.60	1.53	9.13	0.05	0.103	6.3	2.0	4.3
PACS	0.44	67.59	1.63	24.60	5.74	0.364	3.8	1.2	2.6
PAC-NUT	2.63	79.57	1.25	16.50	0.05	0.207	6.0	5.3	0.7

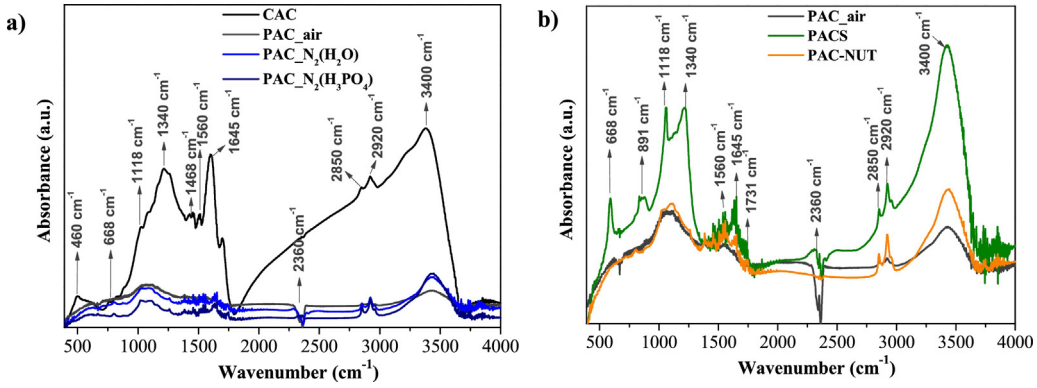

Fig. 3. FTIR spectra of the tested adsorbents.

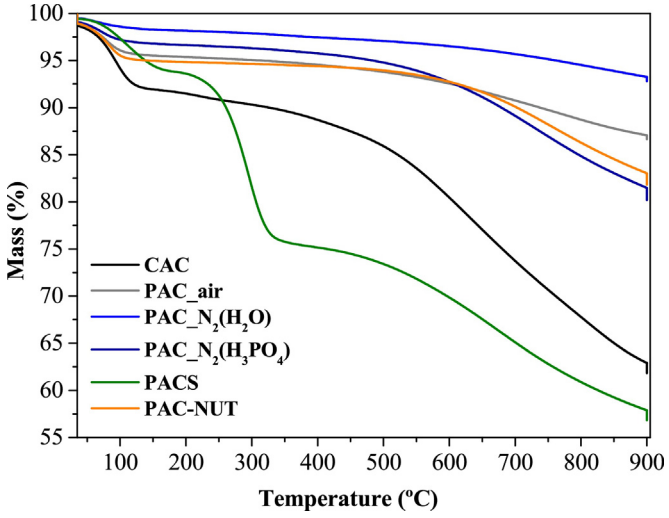

Fig. 4. TG analysis of the tested adsorbents.

ment to those reported in the literature studying activated carbons obtained from biomass wastes [34].

3.1.3. Morphological characterization of the activated carbons

The morphological properties of the synthesized activated carbons have been studied by SEM micrographs (Fig. 5), providing complementary information to the textural properties of the materials.

The more opened-porous structure of CAC activated carbon (Fig. 5a) can be attributed to the wide pore size distribution of the carbon, with a high quantity of pores in the mesoporous range, in accordance to the previous discussion about textural properties. On the other hand, a surface damage, may be attributed to the severe treatment conditions, could be observed in SEM micrographs of PACS and PAC-NUT (Fig. 5e–f, respectively).

3.2. Kinetic adsorption tests. Modeling of the experimental data

Kinetic adsorption experiments were carried out in order to evaluate the kinetic rate of 4-NP adsorption onto the synthesized adsorbents. In Fig. 6 is depicted 4-NP adsorption capacity versus operation time.

Adsorption equilibrium onto CAC activated carbon was attained in 8 h, revealing the fastest kinetic adsorption among the tested systems. This can be attributed to its opened-textural structure, high S_{BET} and pore size, compared to physically-activated carbons. As it has been reported in the literature, 4-NP is a molecule showing high mobility and small size [35], obtaining high adsorption rates onto high surface area-activated carbons.

Physically-activated carbons showed long equilibrium times (48 h) due to their strong microporous character, with highly narrow PSD and small pore size. The treatment with H_2SO_4 (PACS) increased the acidic functionalities content on the carbon surface, mainly thiol, sulphoxide and/or sulphone groups, which decompose releasing SO_2 species and prevailing over carboxylic acids, lactones, phenol and quinone groups [36]. High hydrophilic character of PACS carbon disfavored the adsorption of 4-NP, suggesting that the competition between water and pollutant adsorbing in pores is mainly responsible of the observed decreasing in the adsorption capacity. This led to a slow adsorption rate (96 h) and a very low affinity toward 4-NP molecule.

Generally, it has been widely reported in the literature that basic carbons show high affinity toward phenolic compounds [37]. Thus, PAC-NUT showed the best adsorption behavior ($q_{4\text{-NP}}$ = 35 mg g^{-1} at equilibrium time of 4 h). The treatments with nitric acid and subsequent urea solution originated an increasing in the nitrogen content and a decrease of the oxygenated functionalities on the carbon surface, inferring that some carboxylic acid groups were suppressed by the incorporation of nitrogen functionalities (cyano or amine groups).

The modeling of the experimental kinetic data was assessed by using pseudo-first-order and pseudo-second order equations. Pseudo-first order or Lagergren's model [38] is given by Eq. (1).

$$q = q_e \cdot (1 - e^{-k_1 \cdot t}) \quad (1)$$

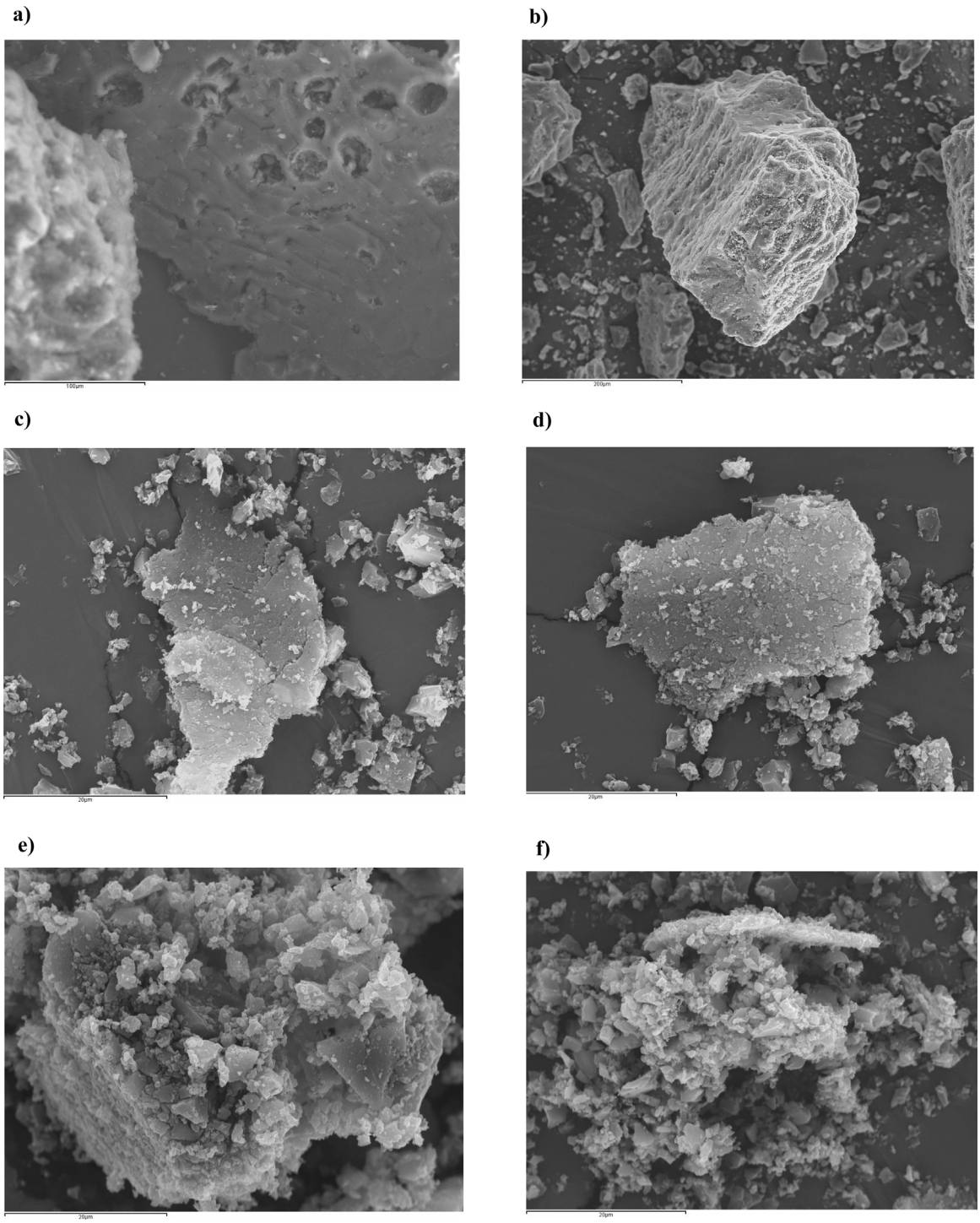

Fig. 5. SEM micrographs of the tested activated carbons: (a) CAC; (b) PAC_air; (c) PAC_N_2(H_2O); (d) PAC_N_2(H_3PO_4); (e) PACS; (f) PAC-NUT.

where q_e and q (mg g^{-1}) are the equilibrium adsorption capacity and the adsorption capacity at time t, respectively; k_1 (min^{-1}) is the pseudo-first-order model rate constant.

Pseudo-second order equation [39] is given by Eq. (2).

$$q = \frac{q_e^2 \cdot k_2 \cdot t}{1 + q_e \cdot k_2 \cdot t} \quad (2)$$

where q_e and q (mg g^{-1}) are the equilibrium adsorption capacity and the adsorption capacity at time t, respectively; k_2 (g mg^{-1} min^{-1}) is the pseudo-second-order rate constant.

The kinetic parameters obtained for both models, and the corresponding correlation coefficients (R^2, SSE, Eq. (3)), this latter as the sum of the square of the residuals minimized in the fitting of the non-linearized equations, are shown in Table 3.

$$SSE = \sum (q_{exp} - q_{cal})^2 \quad (3)$$

where q_{exp} and q_{cal} are the experimental and calculated adsorption capacity values, respectively.

Both pseudo-first order and pseudo-second order models showed good fitting to the experimental data. However, higher R^2

Table 3
Kinetic adsorption data predicted by pseudo-first order and pseudo-second order models for adsorption of 4-NP by carbonaceous materials.

Carbon	Pseudo-first order kinetic					Pseudo-second order kinetic			
	q_e exp (mg g^{-1})	q_e cal (mg g^{-1})	k_1 (min^{-1})	R^2	SSE	q_e cal (mg g^{-1})	k_2 (g mg^{-1} min^{-1})	R^2	SSE
CAC	27.3	27.3	0.205	0.9475	91.3	27.2	0.0061	0.9996	32.8
PAC_air	38.7	38.7	0.050	0.9386	521.5	38.6	0.0005	0.9988	259.5
PAC_N$_2$(H$_2$O)	38.3	38.3	0.034	0.9197	634.9	38.2	0.00043	0.9990	340.4
PAC_N$_2$(H$_3$PO$_4$)	38.1	38.1	0.031	0.9108	662.1	37.9	0.00042	0.9988	358.3
PACS	35.6	35.6	0.001	0.9203	621.3	33.3	8.7×10^{-5}	0.9646	408.5
PAC-NUT	38.4	38.4	0.059	0.9754	60.4	38.3	0.0012	0.9999	24.0

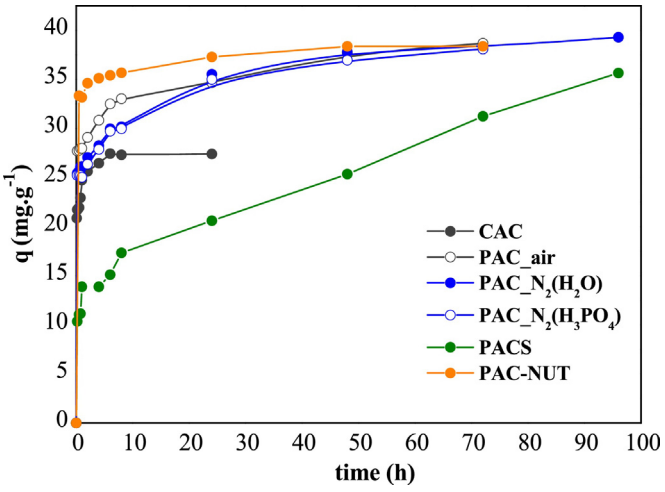

Fig. 6. Experimental adsorption kinetic curves of 4-NP onto the tested adsorbents.

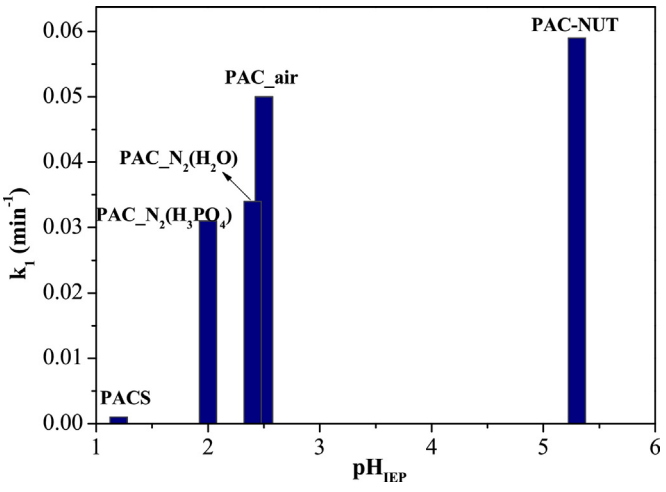

Fig. 7. Pseudo-first kinetic rate constants vs. isoelectric point for the physically-activated carbons (original and modified carbons).

values were obtained for the pseudo-second order model, especially high for the adsorption onto PAC-NUT activated carbon. The literature establishes that the suitability of pseudo-second order model suggesting that the adsorption process is governed by chemisorption forces, that is, by the establishment of valent bonds between surface of the adsorbent and adsorbate, as it will be discussed further.

In general, pseudo-first and pseudo-second order models accord to physical and chemical adsorption domination, respectively, but the division between them is not so clear and further studies are necessary to discuss this aspect.

Similar results have been found by Tang et al. [40] studying the adsorption of 4-NP onto carbon fibers and by Ahmaruzzaman and Laxmi Gayatri [41] on the study of 4-NP removal by activated carbon obtained from jute stick.

Attending to the experimental results, textural properties of the tested carbons are not seem highly influencing on the kinetic rate; so, it seems that the acidity/basicity properties of the carbon materials play a critical role on the adsorption rate. Thus, pH_{IEP} values of the physically-activated carbons can be correlated to k_1 constant (Fig. 7).

From the figure, it can be deduced that the adsorption rate is strongly dependent on the chemical surface properties of the activated carbon; thus, the determined apparent rate constant of 4-NP adsorption onto PAC-NUT was 0.06 min^{-1}, which is 60 times higher than that achieved by PACS.

3.3. Equilibrium adsorption tests. Modeling of the experimental data

From the equilibrium adsorption tests could be inferred that the surface chemistry of the activated carbons plays an important role on the adsorption performance, as detailed above. The adsorption

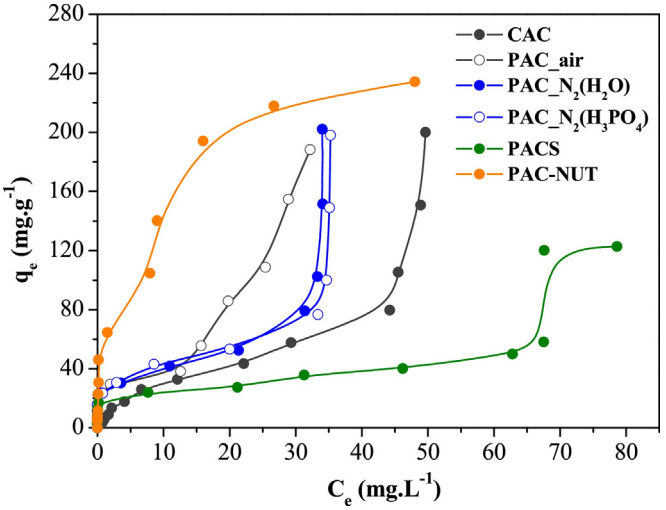

Fig. 8. Experimental adsorption isotherms of 4-NP onto the tested adsorbents.

isotherms of all the studied systems can be classified as L-3 or III type isotherms, according to Giles classification [42] (Fig. 8).

A type III isotherm appears when the binding energy for the first layer is lower than the binding energy between adsorbate molecules. This assumption will be confirmed below through the adsorption modeling of the experimental data.

Double – or more – sigmoid adsorption isotherms are indicating that the energy of adsorption is concentration dependent. So, it can be observed a small initial plateau followed by a sudden rise in the curve at higher aqueous concentration [43]. This rise represents a reorientation of the adsorbed molecules in a direction of a more dense packing because such a reorganization would allow more

Table 4
BET, GAB, Langmuir and Freundlich model parameters for the adsorption of 4-NP by carbonaceous materials.

Carbon	BET model				GAB model			
	q_s (mg g^{-1})	C_{BET} (L mg^{-1})	C_s (mg L^{-1})	SSE	q_m (mg g^{-1})	K_1 (L mg^{-1})	K_2 (L mg^{-1})	SSE
CAC	19.4	40.9	55.4	1328	16.3	928.8	0.018	1945
PAC_air	38.4	683.6	40.0	1393	38.4	17.1	0.025	1393
PAC_N_2(H_2O)	14.6	5.3×10^5	37.4	4440	14.6	6534	0.026	4440
PAC_N_2(H_3PO_4)	7.0	5.3×10^5	36.7	5149	7.0	6536	0.027	5149

Carbon	Langmuir model			Freundlich model		
	q_{sat} (mg g^{-1})	b (L mg^{-1})	SSE	K_F (L g^{-1})	n_F	SSE
PAC-NUT	279.1	0.1	4484	60.6	2.7	2456

space for adsorption. This assumption is in accordance to the relation between 4-NP molecular size (0.684 nm × 0.417 nm [44]) and the average pore width of the tested adsorbent materials. According to Pelekani and Snoeyink [45], the average pore size of the adsorbent should be above 1.2 times of the second widest dimension of the adsorbate molecule to allow effective adsorption. In this work, the pore width-molecular size proportion was found to be in the range from 3 to 6. Since the occurrence of steric hindrance is not expectable, the reaccommodation of the adsorbate in the widest pores is probably generating the sigmoid-type isotherms.

The initial part of the adsorption isotherm is indicating a low interaction between 4-NP and the solid surface at low concentrations. However, as the concentration in the liquid phase increased, adsorption was more readily, occurring multilayer or aggregate formation. This behavior is namely as cooperative adsorption, a synergistic effect with the adsorbed molecules facilitating the adsorption of additional molecules from the aqueous solution, as result of the important role of adsorbate–adsorbate interactions in the adsorption process [46].

Thus, at low aqueous concentration range, high 4-NP molecule affinity toward PAC-NUT carbon was found, so it could be established that the basic surface groups favor the adsorption of 4-NP due to π–π interactions between the carbon surface and the adsorbate molecule. Accordingly, the adsorption onto the chemically-activated carbon was hindered due to its more hydrophilic character, which maybe originates the formation of water molecules clusters located in the carbon porous structure and the blockage of some pore entrances (solvent effect). Through this phenomenon, some pores may be inaccessible to the formed phenol-water aggregates [47].

Such sigmoid trend in the adsorption isotherms has been reported for phenol adsorption on some activated carbons by Terzyk [36], which postulated that the adsorption mechanism of phenolic compounds is based on the formation of donor-acceptor complexes between the oxygenated surface functionalities (electron donors) and the aromatic ring of phenol acting as acceptor. According to Terzyk, carboxylic groups, i.e., the most acidic, play an important role in the adsorption of phenolic compounds at small concentration, dramatically decreasing the adsorption capacity.

Indeed, phenolic compounds, due to their planar shape and delocalized π-bonds, interact strongly with the adsorbent surface, by the so-called π–π interactions, causing a reorientation of the molecule into the pores. This implies that the adsorption is occurring on surface active centers located in larger micropores (or in mesopores), leading to the changes observed in the shape of the isotherms. Thus, the adsorbed molecules generate binding interactions with the molecules in solution, increasing the adsorption capacity at higher concentrations.

Furthermore, it has also been reported that oxygen and nitrogen groups of 4-NP molecule react with both oxygenated and nitrogenated-functionalities on the carbon surface (PAC-NUT), resulting in the formation of covalent bonding [48,49], which is in accordance to the good fitting found to the pseudo-second order model.

Zhu and Gu [50] found aggregate formation on the adsorption processes, indicating that this type of adsorption involves two phases; in the first phase, adsorption is occurring on the carbon surface, and in the second phase, the interaction between the adsorbed molecules is involved.

Meanwhile, according to pK_a value of 4-NP (7.15 [44]) and pH_{PZC} and pH_{IEP} of the carbons, ranging from 1.0 and 6.0, it is expected that electrostatic forces are not involved in 4-NP adsorption process.

BET model was applied to adequately describe the multi-layer adsorption isotherms [51,52]:

$$q_e = \frac{q_s \cdot C_{BET} \cdot C_e}{(C_s - C_e) \cdot \left[1 + (C_{BET} - 1) \cdot (C_e/C_s)\right]} \quad (4)$$

where q_e (mg g^{-1}) and C_e (mg L^{-1}) are adsorption capacity and aqueous-phase concentration at equilibrium, respectively; C_{BET} (L mg^{-1}) is the characteristic parameter of BET equation; C_s (mg L^{-1}), the saturation concentration on the monolayer and q_s (mg g^{-1}), the theoretical adsorption capacity following BET equation.

Thus, a modified form of BET model is the Guggenheim-Anderson-De Boer (GAB) equation, which postulates that the state of the adsorbate molecules on the second and subsequent layers is equal between them, but it is different to those molecules that are in liquid phase. Accordingly, in this case, the adsorption is occurring on a finite number of layers, whereas the BET equation deals with an infinite number [53]. GAB isotherm model is expressed as presented in Eq. (5).

$$q_e = \frac{q_m \cdot K_1 \cdot C_e}{(1 - K_2 \cdot C_e) \cdot [1 + (K_1 - K_2) \cdot C_e]} \quad (5)$$

where q_e (mg g^{-1}) is the equilibrium adsorption capacity; C_e (mg L^{-1}) is the equilibrium concentration in the aqueous phase; q_m (mg g^{-1}) is the maximum adsorption capacity on the first layer and K_1 and K_2 (L mg^{-1}) are the equilibrium constants for the first and second layer, respectively.

Both BET and GAB models satisfactorily reproduced the experimental adsorption data of the non-modified activated carbons. The model parameters are summarized in Table 4, including SSE values.

K_1 parameters were much higher than K_2 for all the studied systems. This can be attributed to the fact that the adsorbate is more strongly attached to the carbon surface at low concentrations and weak lateral interactions occurred at higher aqueous concentrations [54].

Thus, Langmuir model [55], suitable for monolayer adsorption (Eq. (6)), and Freundlich equation [56], commonly applied to heterogeneous processes (Eq. (7)), were used to describe the adsorption data of 4-NP onto PAC-NUT. Therefore, the experimental PACS adsorption data were not fitted satisfactorily to none of

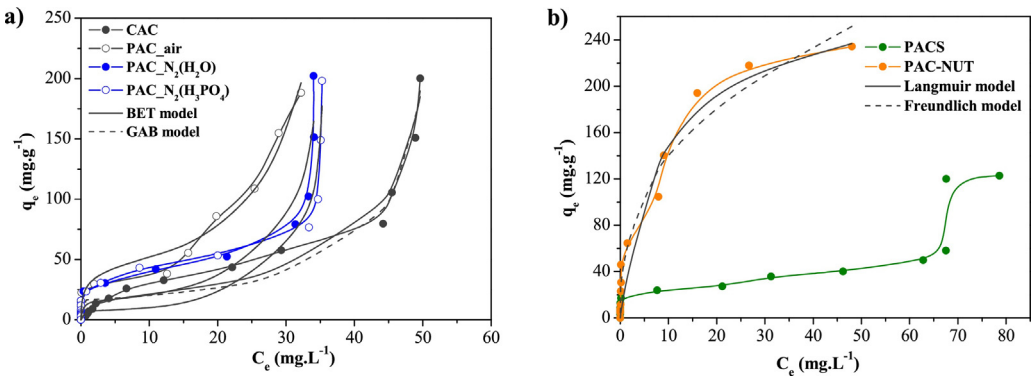

Fig. 9. Experimental and theoretical adsorption isotherms of 4-NP onto (a) non-modified and (b) modified carbon materials.

Table 5
Results on adsorption of phenolic compounds by lignocellulosic-activated carbons reported in the literature.

Adsorbent	Contaminant	q_{exp} (mg g^{-1})	Reference
Apricot stones-based activated carbon	Phenol	150.0	[55,58]
	4-Nitrophenol	145.0	
Activated carbon derived from rice straw	4-Chlorophenol	24.0	[56,59]
Physically and chemically-activated carbons from jute and coconut fibers	Phenol	150.0	[57,60]
		75.0	
		180.0	
		112.0	
Activated carbon from date pits (activated with H_3PO_4)	4-Nitrophenol	108.7	[25,35]
Microwave-assisted activated carbons from wood chips	Phenol	175.0	[58,61]
Activated carbon prepared from waste tea	Phenol	37.0	[59,62]
Physically-activated carbon from peach stones and further treated with urea (PAC-NUT)	4-Nitrophenol	234.3	This work

the tested models, e.g., BET, GAB, Langmuir, Freundlich and Sips equations.

$$q_e = \frac{q_{sat} \cdot b \cdot C_e}{(1 + b \cdot C_e)} \quad (6)$$

$$q_e = K_F \cdot C_e^{1/n_F} \quad (7)$$

where q_e (mg g^{-1}) is the equilibrium adsorption capacity; C_e (mg L^{-1}), the equilibrium concentration; q_{sat} (mg g^{-1}) is the maximum adsorption capacity on the monolayer; b (L mg^{-1}) is the adsorption equilibrium constant for Langmuir model; K_F (L g^{-1}) is the adsorption affinity coefficient and $1/n_F$ indicates the intensity of the adsorption process in the Freundlich equation. Both Langmuir and Freundlich parameters are shown in Table 4.

The experimental data obtained for the non-modified carbons and the non-linearized model fitting are plotted in Fig. 9a, while experimental and theoretical adsorption data of modified-carbons are depicted in Fig. 9b.

PAC-NUT adsorption data were better described by Freundlich model. $1/n_F$ value was found to be less than 1, suggesting that 4-NP adsorption on PAC-NUT carbon is a favorable process. Good correlation of both Langmuir and Freundlich models to adsorption data of phenolic compounds has been widely reported in the literature [47,57].

Several experimental results from studies on the adsorption of phenolic compounds by lignocellulosic-activated carbons are summarized in Table 5. It was found that the results obtained for PAC-NUT activated carbon are highly competitive in the removal of 4-NP from aqueous solution.

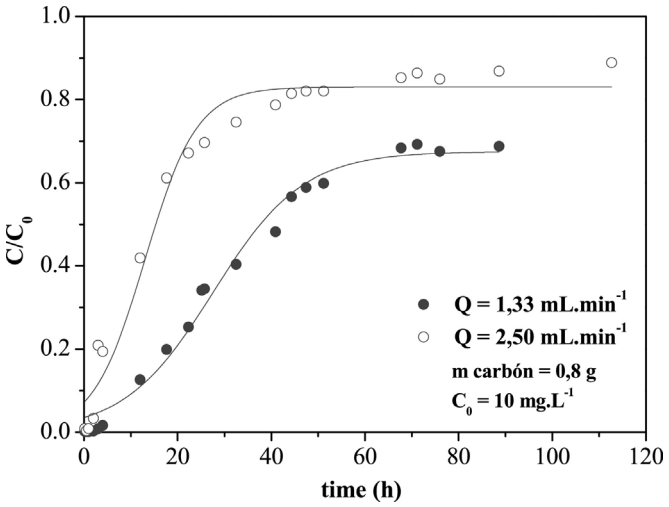

Fig. 10. Breakthrough curves of 4-NP onto PAC_air adsorbent at the operation conditions: C_0 = 10 mg L^{-1}, Q = 2.0 mL min^{-1} and mass of adsorbent = 0.8 g.

3.4. Fixed-bed adsorption experiments. Estimation of adsorption parameters

Fixed-bed column adsorption studies of 4-NP were accomplished with PAC_air activated carbon. Breakthrough curves at different volumetric flow rates (Q = 1.33 and 2.50 mL min^{-1}), C_0 = 10.0 mg L^{-1} of 4-NP and 0.8 g of activated carbon were obtained (Fig. 10). Generally, flatter profiles for both breakthrough curves were observed, mainly attributed to a high influence of the mass transfer resistance in the adsorption process.

Breakthrough times (t_b), calculated at C/C_0 = 0.05, were found to be 6.4 and 2.1 h (Q = 1.33, 2.50 mL min^{-1}), respectively. The maxi-

Table 6
Adsorption capacities, MTZ, FBU and removal percentage for adsorption of 4-NP adsorption by carbonaceous materials.

Q (mL min^{-1})	t_b (h)	t_s (h)	q_b (mg g^{-1})	q_s (mg g^{-1})	MTZ (cm)	FBU	Y (%)
1.33	6.4	88.7	4.4	20.4	6.3	0.21	68.4
2.50	2.1	88.7	3.3	27.2	7.0	0.12	85.1

mum saturation obtained in the column operating at 1.33 mL min^{-1} was C/C_0 = 0.69 (t_s = 88.6 h); meanwhile, the adsorption bed working at a flow rate of 2.50 mL min^{-1} reached a C/C_0 value of 0.89, for the same saturation time. This suggested that when the flow rate was higher, the time required to remove the same quantity of pollutant was shorter due to the bed was saturated earlier. Thus, at higher volumetric flow rate, a decreasing in the breakthrough time was observed, and resulting in a steeper breakthrough curve (Fig. 10), indicating a decrease in the mass transfer resistance of the adsorption process [63].

Adsorption parameters, e.g., breakthrough time (t_b), saturation time (t_s), adsorption capacity at breakthrough time (q_b, mg g^{-1}), adsorption capacity at saturation time (q_s, mg g^{-1}), mass transfer zone length (MTZ, cm), fractional bed utilization (FBU, dimensionless) and adsorbate removal percentage at breakthrough time (Y, %) were determined and summarized in Table 6.

It can be concluded that at a lower flow rate, the residence time of the adsorbate in the column is higher and thus, the adsorbent is getting more time to bond with 4-NP molecule efficiently. This resulted in a slight increase in the adsorption capacity at breakthrough time, indicating that the adsorption process is controlled by intra-particle diffusion mass transfer. A similar tendency has been found by other researchers [64,65].

4. Conclusions

In this study, it was found that 4-NP adsorption is highly conditioned by the chemical surface properties of the adsorbent. Accordingly, the best adsorption results, in terms of adsorption capacity and molecule affinity, were those obtained for the more basic activated carbon (PAC-NUT). Additionally, the chemically-activated carbon (CAC) showed the highest specific surface area, total pore volume and pore size values. This carbon, with hydrophilic character, offered good kinetic properties, due to its more opened-porous structure, but low affinity toward 4-NP molecule. Thus, physically-activated carbons showed much more hindered textural properties (totally microporous materials).

Experimental kinetic data were successfully fitted to the pseudo-second order model, suggesting that chemisorption forces could be involved in 4-NP adsorption process. The strong dependency of the adsorption rate on the chemical properties of the adsorbent was corroborated through the relationship between the apparent kinetic rate constants and pH_{IEP} values of the carbons.

The adsorption isotherms showed a sigmoid trend, attributed to a bilayer/multilayer adsorption, being well reproduced by BET and GAB models. Breakthrough curves of 4-NP onto PAC_air at different volumetric flow rates were obtained, showing a latter profile and not a total column saturation. Finally, the breakthrough curve obtained at high flow rate (Q = 2.5 mL min^{-1}) showed a higher slope, attributed to a decreasing in the mass transfer resistance.

Acknowledgements

The authors would like to thank the financial support of Ministry of Economía and Competitividad of Spain (Contract CTQ2014-59011-R REMEWATER and TRAGUANET Network CTM2014-53485-REDC), the Regional Government of Madrid provided through Project REMTAVARES S2013/MAE-2716 and the European Social Fund, and Project POCI-01-0145-FEDER-006984 – Associate Laboratory LSRE-LCM, funded by FEDER through COMPETE2020 – Programa Operacional Competitividade e Internacionalização (POCI) – and by national funds through FCT – Fundação para a Ciéncia e a Tecnologia. M. Martin-Martinez acknowledges financial support from the FCT Postdoctoral grant SFRH/BPD/108510/2015. S. Álvarez-Torrellas acknowledges also the funding provided by the Spanish Ministry of Economy and Competitiveness (MINECO) through Juan de la Cierva-Formacion Contract.

Appendix A. Supplementary data

Supplementary data associated with this article can be found, in the online version, at http://dx.doi.org/10.1016/j.apsusc.2017.04.054.

References

[1] M. Sarkar, P.K. Acharya, Use of fly ash for the removal of phenol and its analogues from contaminated water, Waste Manage. 26 (2006) 559–570.
[2] J.-Q. Jiang, C. Cooper, S. Ouki, Comparison of modified montmorillonite adsorbents. Part I: Preparation, characterization and phenol adsorption, Chemosphere 47 (2002) 711–716.
[3] A. Bhatnagara, M. Sillanpääb, Utilization of agro-industrial and municipal waste materials as potential adsorbents for water treatment – a review, Chem. Eng. J. 157 (2010) 277–296.
[4] T. Heberer, Occurrence, fate, and removal of pharmaceutical residues in the aquatic environment: a review of recent research data, Toxicol. Lett. 131 (2002) 5–17.
[5] M.J. Ahmed, S.K. Theydan, Equilibrium isotherms, kinetics and thermodynamics studies of phenolic compounds adsorption on palm-tree fruit stones, Ecotoxicol. Environ. Saf. 84 (2012) 39–45.
[6] P.J. Smeets, J.S. Woertink, B.F. Sels, E.I. Solomon, R.A. Schoonheydt, Transition-metal ions in zeolites: coordination and activation of oxygen, Inorg. Chem. 49 (2010) 3573–3583.
[7] M. Wisniewska, V. Bogatyrov, I. Ostolska, K. Szewczuk-Karpisz, K. Terpilowski, A. Nosal-Wiercinska, Impact of poly(vinyl alcohol) adsorption on the surface characteristics of mixed oxide Mn_xO_y-SiO_2, Adsorption 22 (2016) 417–423.
[8] V.K. Gupta, A. Nayak, S. Agarwal, Bioadsorbents for remediation of heavy metals: current status and their future prospects, Environ. Eng. Res. 20 (2015) 1–18.
[9] M.A. Chayid, M.J. Ahmed, Amoxicillin adsorption on microwave prepared activated carbon from *Arundo donax* Linn: isotherms, kinetics, and thermodynamics studies, J. Environ. Chem. Eng. 3 (2015) 1592–1601.
[10] D. Duranoglu, A.W. Trochimczuk, U. Beker, A comparison study of peach stone and acrylonitrile-divinylbenzene copolymer based activated carbons as chromium (VI) sorbents, Chem. Eng. J. 165 (2010) 56–63.
[11] J.V. Flores-Cano, M. Sánchez-Polo, J. Messoud, I. Velo-Gala, R. Ocampo-Pérez, J. Rivera-Utrilla, Overall adsorption rate of metronidazole, dimetridazole and diatrizoate on activated carbons prepared from coffee residues and almond shells, J. Environ. Manage. 169 (2016) 116–125.
[12] P. Nowicki, J. Kazmierczak, R. Pietrzak, Comparison of physicochemical and sorption properties of activated carbons prepared by physical and chemical activation of cherry stones, Powder Technol. 269 (2015) 312–319.
[13] P. Nowicki, J. Kazmierczak-Razna, P. Skibiszewska, M. Wisniewska, A. Nosal-Wiercinska, R. Pietrzak, Production of activated carbons from biodegradable waste materials as an alternative way of their utilisation, Adsorption 22 (2016) 489–502.
[14] M. Wisniewska, P. Nowicki, A. Nosal-Wiercinska, R. Pietrzak, K. Szewczuk-Karpisz, I. Ostolska, D. Sternik, Adsorption of poly(acrylic acid) on the surface of microporous activated carbon obtained from cherry stones, Colloid. Surf. A 514 (2017) 137–145.
[15] Q.-S. Liu, T. Zheng, P. Wang, L. Guo, Preparation and characterization of activated carbon from bamboo by microwave-induced phosphoric acid activation, Ind. Crops Prod. 31 (2010) 233–238.
[16] A.J. Romero-Anaya, M.A. Lillo-Rodenas, C.S.M. Lecea, A. Linares-Solano, Hydrothermal and conventional H_3PO_4 activation of two natural bio-fibers, Carbon 50 (2012) 3158–3169.
[17] M. Turmuzi, W.R.W. Daud, S.M. Tasirin, M.S. Takriff, S.E. Iyuke, Production of activated carbon from candlenut shell by CO_2 activation, Carbon 42 (2004) 453–455.

[18] M.J. Ahmed, S.K. Theydan, Physical and chemical characteristics of activated carbon prepared by pyrolysis of chemically treated date stones and its ability to adsorb organics, Powder Technol. 229 (2012) 237–245.
[19] S. Álvarez-Torrellas, R. García Lovera, N. Escalona, C. Sepúlveda, J.L. Sotelo, J. García, Chemical-activated carbons from peach stones for the adsorption of emerging contaminants in aqueous solutions, Chem. Eng. J. 279 (2015) 788–798.
[20] R.S. Ribeiro, A.M.T. Silva, M.T. Pinho, J.L. Figueiredo, J.L. Faria, H.T. Gomes, Development of glycerol-based metal-free carbon materials for environmental catalytic applications, Catal. Today 240 (2015) 61–66.
[21] I. Ghouma, M.J. Jeguirim, S. Dorge, L. Limousy, C.M. Ghimbeu, A. Ouederni, Activated carbon prepared by physical activation of olive stones for the removal of NO_2 at ambient temperature, C. R. Chim. 18 (2015) 63–74.
[22] H.T. Gomes, S.M. Miranda, M.J. Sampaio, A.M.T. Silva, J.L. Faria, Activated carbons treated with sulphuric acid: catalysts for catalytic wet peroxide oxidation, Catal. Today 151 (2010) 153–158.
[23] R.P. Rocha, J.P.S. Sousa, A.M.T. Silva, M.F.R. Pereira, J.L. Figueiredo, Catalytic activity and stability of multiwalled carbon nanotubes in catalytic wet air oxidation of oxalic acid: the role of the basic nature induced by the surface chemistry, Appl. Catal. B: Environ. 104 (2011) 330–336.
[24] S. Brunauer, P.H. Emmett, E.J. Teller, Adsorption of gases in multimolecular layers, J. Am. Chem. Soc. 60 (1938) 309–319.
[25] M.M. Dubinin, Adsorption in micropores, J. Colloid Interf. Sci. 23 (1967) 487.
[26] S.J. Gregg, K.S.W. Sing, Adsorption, Surface and Porosity, Academic Press, London, 1982.
[27] J.J.M. Orfão, A.I.M. Silva, J.C.V. Pereira, S.A. Barata, I.M. Fonseca, P.C.C. Faria, M.F.R. Pereira, Adsorption of reactive dye on chemically modified activated carbon-influence of pH, J. Colloid Interf. Sci. 296 (2006) 480–489.
[28] K.S.W. Sing, D.H. Everett, R.A.W. Haul, L. Moscou, R.A.W. Pierotti, J. Rouquerol, T. Siemieniewska, Reporting physisorption data for gas/solid systems with special reference to the determination of surface area and porosity, Pure Appl. Chem. 57 (1985) 603–619.
[29] G.-Y. Oh, Y.-W. Ju, M.-Y. Kim, H.-R. Jung, H.J. Kim, W.-J. Lee, Adsorption of toluene on carbon nanofibers prepared by electrospinning, Sci. Total Environ. 393 (2008) 341–347.
[30] C.A. León y León, L.R. Radovic, Effect of thermal and chemical pretreatments on the copper-catalyzed gasification of carbon in air, Abstr. Pap. Am. Chem. Soc. 202 (1991) 967–974.
[31] C.J. Durán-Valle, M. Gómez-Corzo, J. Pastor-Villegas, V. Gómez-Serrano, Study of cherry stones as raw material in preparation of carbonaceous adsorbents, J. Anal. Appl. Pyrolysis 73 (2005) 59–67.
[32] Z.-M. Wang, N. Yamashita, Z.-X. Wang, K. Hoshinoo, H. Kanoh, Air oxidation effects on microporosity, surface property, and CH_4 adsorptivity of pitch-based activated carbon fibers, J. Colloid Interf. Sci. 276 (2004) 143–150.
[33] C. Tangsathitkulchai, Y. Ngernyen, M. Tangsathitkulchai, Surface modification and adsorption of eucalyptus wood-based activated carbons: effects of oxidation treatment, carbon porous structure and activation method, Korean J. Chem. Eng. 26 (2009) 1341–1352.
[34] G.-Z. Zhu, X.-I. Deng, M. Hou, K. Sun, Y.-P. Zhang, P. Li, F.-M. Liang, Comparative study on characterization and adsorption properties of activated carbons by phosphoric acid activation from corncob and its acid and alkaline hydrolysis residues, Fuel Process. Technol. 144 (2016) 255–261.
[35] H. Altaher, A.M. Dietrich, Characterizing o- and p-nitrophenols adsorption onto innovative activated carbon prepared from date pits, Water Sci. Technol. 69 (2014) 31–37.
[36] A.P. Terzyk, Further insights into the role of carbon surface functionalities in the mechanism of phenol adsorption, J. Colloid Interf. Sci. 268 (2003) 301–329.
[37] C. Moreno-Castilla, Adsorption of organic molecules from aqueous solutions on carbon materials, Carbon 42 (2004) 83–94.
[38] H. Yuh-Shan, Citation review of Lagergren kinetic rate equation on adsorption reactions, Scientometrics 59 (2004) 171–177.
[39] M. Nadeem, A. Mahmood, S.A. Shahid, S.S. Shah, A.M. Khalid, G. McKay, Sorption of lead from aqueous solution by chemically modified carbon adsorbents, J. Hazard. Mater. 138 (2006) 604–613.
[40] D. Tang, Z. Zheng, K. Lin, J. Luan, J. Zhang, Adsorption of p-nitrophenol from aqueous solutions onto activated carbon fiber, J. Hazard. Mater. 143 (2007) 49–56.
[41] M. Ahmaruzzaman, S. Laxmi Gayatri, Batch adsorption of 4-nitrophenol by acid activated jute stick char: equilibrium, kinetic and thermodynamic studies, Chem. Eng. J. 158 (2010) 173–180.
[42] C.H. Giles, T.H. MacEwan, S.N. Nakhwa, D. Smith, Studies in adsorption. Part XI: A system of classification of solution adsorption isotherms, and its use in diagnosis of adsorption mechanism and in measurement of specific surface areas of solids, J. Chem. Soc. (1960) 3973–3993.
[43] A.K. Helmy, S.G. de Bussetti, E.A. Ferreiro, Adsorption of quinolone from aqueous solutions by some clays and oxides, Clay. Clay Miner. 31 (1983) 29–36.
[44] Q.-S. Liu, T. Zheng, P. Wang, J.-P. Jiang, N. Li, Adsorption isotherm, kinetic and mechanism studies of some substituted phenols on activated carbon fibers, Chem. Eng. J. 157 (2010) 348–356.
[45] C. Pelekani, V.L. Snoeyink, Competitive adsorption between atrazine and methylene blue on activated carbon: the importance of pore size distribution, Carbon 38 (2000) 1423–1436.
[46] V. Gómez, M.S. Larrechi, M.P. Callao, Kinetic and adsorption study of acid dye removal using activated carbon, Chemosphere 69 (2007) 1151–1158.
[47] N.G. Rincón-Silva, J.C. Moreno-Piraján, L.G. Giraldo, Thermodynamic study of adsorption of phenol, 4-chlorophenol, and 4-nitrophenol on activated carbon obtained from eucalyptus seed, J. Chem. (2015) 1–12.
[48] A. Morsli, A. Benhamou, J.-P. Basly, M. Baudu, Z. Derriche, Mesoporous silicas: improving the adsorption efficiency of phenolic compounds by the removal of amino group from functionalized silicas, RSC Adv. 5 (2015) 41631–41638.
[49] M. Martín-Martínez, R.S. Ribeiro, B.F. Machado, P. Serp, S. Morales-Torres, A.M.T. Silva, J.L. Figueiredo, J.L. Faria, H.T. Gomes, Role of nitrogen doping on the performance of carbon nanotube catalysts: a catalytic wet peroxide oxidation application, Chem. Cat. Chem. 8 (2016) 2068–2078.
[50] B.Y. Zhu, T. Gu, General isotherm equation for adsorption of surfactants at solid/liquid interfaces, J. Chem. Soc., Faraday Trans. 85 (1989) 3813–3817.
[51] S. Brunauer, P.H. Emmett, E. Teller, Adsorption of gases in multimolecular layers, J. Am. Chem. Soc. 60 (1938) 309–319.
[52] K.Y. Foo, B.H. Hameed, Insights into the modeling of adsorption isotherm systems, Chem. Eng. J. 156 (2010) 2–10.
[53] L.M. Cotoruelo, M.D. Marqués, J. Rodríguez-Mirasol, J.J. Rodríguez, T. Cordero, Cationic dyes removal by multilayer adsorption on activated carbons from lignin, J. Porous Mater. 18 (2011) 693–702.
[54] P. Girods, A. Dufour, V. Fierro, Y. Rogaume, C. Rogaume, A. Zoulalian, A. Celzard, Activated carbons prepared from wood particleboard wastes: characterisation and phenol adsorption capacities, J. Hazard. Mater. 166 (2009) 491–501.
[55] I. Langmuir, The adsorption of gases on plane surfaces of glass, mica and platinum, J. Am. Chem. Soc. 40 (1918) 1361–1403.
[56] M. Jaroniec, Adsorption on heterogeneous surfaces: the exponential equation for the overall adsorption isotherm, Surf. Sci. 50 (1975) 553–564.
[57] H. Ding, X. Li, J. Wang, X. Zhang, C. Chen, Adsorption of chlorophenols from aqueous solutions by pristine and surface functionalized single-walled carbon nanotubes, J. Environ. Sci. 43 (2016) 187–198.
[58] B. Petrova, T. Budinova, B. Tsyntsarski, V. Kochkodan, Z. Shkavro, N. Petrov, Removal of aromatic hydrocarbons from water by activated carbon from apricot stones, Chem. Eng. J. 165 (2010) 258–264.
[59] Y.-H. Shih, Y.-F. Su, R.-Y. Ho, P.-H. Su, C.-Y. Yang, Distinctive sorption mechanisms of 4-chlorophenol with black carbons as elucidated by different pH, Sci. Total Environ. 433 (2012) 523–529.
[60] N.-H. Phan, S. Rio, C. Faur, L. Le Coq, P. Le Cloirec, T.H. Nguyen, Production of fibrous activated carbons from natural cellulose (jute, coconut) fibers for water treatment applications, Carbon 44 (2006) 2569–2577.
[61] P.S. Thue, M.A. Adebayo, E.C. Lima, J.M. Sieliechi, F.M. Machado, G.L. Dotto, J.C.P. Vaghetti, S.L.P. Dias, Preparation, characterization and application of microwave-assisted activated carbons from wood chips for removal of phenol from aqueous solution, J. Mol. Liq. 223 (2016) 1067–1080.
[62] Y. Gokce, Z. Aktas, Nitric acid modification of activated carbon produced from waste tea and adsorption of methylene blue and phenol, Appl. Surf. Sci. 313 (2014) 352–359.
[63] S. Banerjee, G.C. Sharma, R.K. Gautam, M.C. Chattopadhyaya, S.N. Upadhyay, Y.C. Sharma, Removal of malachite green, a hazardous dye from aqueous solutions using *Avena sativa* (oat) hull as a potential adsorbent, J. Mol. Liq. 213 (2016) 162–172.
[64] G. Nazari, H. Abolghasemi, M. Esmaieli, E.S. Pouya, Aqueous phase adsorption of cephalexin by walnut shell-based activated carbon: a fixed-bed column study, Appl. Surf. Sci. 375 (2016) 144–153.
[65] S. Chen, Q. Yue, B. Gao, Q. Li, X. Xu, K. Fu, Adsorption of hexavalent chromium from aqueous solution by modified corn stalk: a fixed-bed column study, Bioresour. Technol. 113 (2012) 114–120.